



**HAL**  
open science

# THERMOELASTIC GRATING FOR NON-DESTRUCTIVE TESTING BY LASER ULTRASONICS

M Karam, Meriem Chrifi Alaoui, Frédéric Jenot, M Baher, Rabih Tauk,  
Mohammadi Ouaftouh, Jihane Jabbour, Marc Duquennoy, Jamal Assaad

► **To cite this version:**

M Karam, Meriem Chrifi Alaoui, Frédéric Jenot, M Baher, Rabih Tauk, et al.. THERMOELASTIC GRATING FOR NON-DESTRUCTIVE TESTING BY LASER ULTRASONICS. Forum Acusticum, Sep 2023, TURIN, Italy. 10.61782/fa.2023.0370 . hal-04342644

**HAL Id: hal-04342644**

**<https://hal.science/hal-04342644>**

Submitted on 13 Dec 2023

**HAL** is a multi-disciplinary open access archive for the deposit and dissemination of scientific research documents, whether they are published or not. The documents may come from teaching and research institutions in France or abroad, or from public or private research centers.

L'archive ouverte pluridisciplinaire **HAL**, est destinée au dépôt et à la diffusion de documents scientifiques de niveau recherche, publiés ou non, émanant des établissements d'enseignement et de recherche français ou étrangers, des laboratoires publics ou privés.

# THERMOELASTIC GRATING FOR NON-DESTRUCTIVE TESTING BY LASER ULTRASONICS

M. Karam<sup>1,2\*</sup>    M. Chrifi Alaoui<sup>1</sup>    F. Jenot<sup>1</sup>    M. Baher<sup>1</sup>    R. Taouk<sup>2</sup>  
M. Ouaftouh<sup>1</sup>    J. Jabour<sup>2</sup>    M. Duquennoy<sup>1</sup>    J. Assaad<sup>1</sup>

<sup>1</sup> Univ. Polytechnique Hauts-de-France, CNRS, Univ. Lille, UMR 8520 - IEMN - Institut d'Electronique de Microélectronique et de Nanotechnologie, F-59313 Valenciennes, France

<sup>2</sup> Uni. Libanaise, Laboratoire de Physique Appliquée (LPA)-Faculté des sciences 2, Fanar, Liban

## ABSTRACT

Ultrasonic Non-Destructive Testing (NDT) uses many types of sources mostly based on piezoelectric transducers. This paper focuses on the generation and detection of acoustic waves by Laser Ultrasonics which is a well-known non-contact inspection method. More precisely, the main goal of this work is to analyze the interaction between a flaw and Rayleigh waves simultaneously excited by a grating of thermoelastic line sources. Experimentally, a pulsed Nd:YAG laser, combined with different optical devices is used for ultrasound excitation in an aluminum sample with a surface defect. Moreover, the normal displacement of Rayleigh waves is detected by a Mach-Zehnder type interferometer. The results obtained using different configurations are compared to determine the advantages of each of them for NDT. A finite element model also allows to confirm the interpretation of the complex phenomena studied.

**Keywords:** *Laser ultrasonics, Non-Destructive Testing, Rayleigh waves, Flaws.*

## 1. INTRODUCTION

Laser ultrasonics is a non-destructive testing method that uses laser to generate and detect ultrasonic waves in

\*Corresponding author: [Maha.karam@uphf.fr](mailto:Maha.karam@uphf.fr).

**Copyright:** ©2023 First author et al This is an open-access article distributed under the terms of the Creative Commons Attribution 3.0 Unported License, which permits unrestricted use, distribution, and reproduction in any medium, provided the original author and source are credited.

metallic and plastic materials [1]. Compared to conventional ultrasonic methods, laser ultrasonics provides many advantages such as higher spatial resolution, the ability to test structures with complex geometries and being contactless [2]. This method has become extensively used in various applications, especially for detecting and characterizing defects in different materials. Over the past decades, lasers have been widely employed as a powerful instrument to generate and detect ultrasound. The Nd:YAG pulsed laser is frequently used to excite these waves either through thermoelastic or ablation mode [1,3].

In an isotropic, homogeneous, and semi-infinite solid, a surface acoustic wave, first described by Lord Rayleigh [4], can propagate. This Rayleigh wave has an elliptical polarization and propagates with an exponentially decreasing amplitude from the surface to the depth of the solid. In most Laser ultrasounds applications, the Rayleigh wave is generated by a thermoelastic line source for material characterization and defect detection [5]. In this work, we are interested in the simultaneous generation of multiple Rayleigh waves for structures non-destructive testing. An experimental setup for obtaining multiple line sources is implemented.

This article focuses on the analysis of the interaction between Rayleigh waves generated by laser ultrasonics and surface defects on an aluminum sample, through both numerical and experimental investigations. In the first part, the propagation velocity and directivity of the Rayleigh wave in aluminum for a line source are determined based on theoretical considerations. The second part describes the generation of Rayleigh waves on the surface of the sample by the Finite Element Method, ex-

cited by a grating of thermoelastic line sources, and the resulting outcomes. In the third part, a defect with well-known characteristics is created on the sample's surface and an experimental study is conducted to measure the Rayleigh wave propagation velocity in the case of both single and multiple line sources. Finally, the approximate position of the defect and certain dimensions of the sample are determined.

## 2. CHARACTERISTICS OF RAYLEIGH WAVE

Rayleigh waves are a type of guided waves that propagate along the surface of a material, and they are frequently used for non-destructive testing to detect surface flaws. When a Rayleigh wave interacts with a surface defect, such as a discontinuity or crack, the wave is scattered. This scattering phenomenon provides valuable information about the position and size of the defect, which makes Rayleigh waves an effective tool for detecting surface defects in materials.

### 2.1 Propagation velocity

The propagation velocity of a Rayleigh wave in a homogeneous and isotropic material can be theoretically approximated using the following relation [6]:

$$V_R = \frac{(0,87 + 1,12\nu)}{(1 + \nu)} \cdot V_T \quad (1)$$

Where:

$V_R$ : Rayleigh wave velocity,

$V_T$ : Transverse wave velocity,

$\nu$ : Poisson's ratio of the material.

For an aluminum sample, the Poisson's ratio is 0.33 [7] and the propagation velocity of the transverse wave is equal to 3130 m/s [8]. Therefore, Eq. 1 gives a Rayleigh wave propagation velocity in an aluminum sample of approximately 2917 m/s. This theoretical value will be compared to the velocity analysis through the modeling and experimental study.

### 2.2 Directivity

The Rayleigh wave generated by a thermoelastic line source is characterized by its directional aspect. Indeed, this wave mainly propagates in the direction perpendicular to the center of the line [4]. Furthermore, the length of the line source has a direct influence on the wave's directivity pattern [9]. This one can be graphically represented

as a polar plot, which shows the relative amplitude of the waves as a function of the observation angle compared to the line source. The directivity diagram of the Rayleigh wave, assuming a 2 mm-long line source in a thermoelastic regime at a frequency of 6 MHz, is presented in Figure 1.

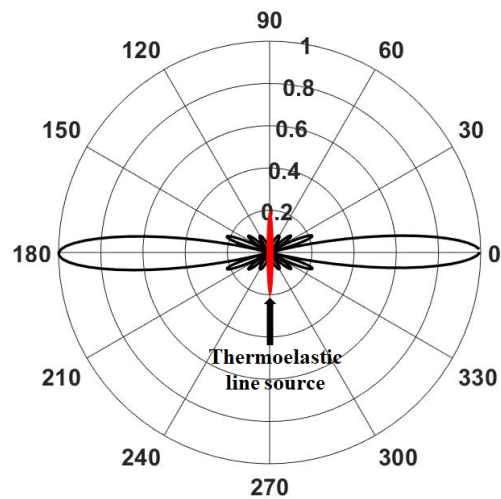


**Figure 1.** Directivity diagram of a Rayleigh wave generated by a line source with a length of 2 mm in aluminum.

## 3. FINITE ELEMENT METHOD

Many articles in the literature concentrate on modeling the generation of ultrasound by laser and the interaction of these waves with a defect, using the finite element method (FEM) [10]. The present study aims to describe the generation of Rayleigh waves on the surface of an aluminum sample with multiple line sources. In order to conduct the analysis, a FEM model is developed. The first part of this section will introduce the modeling parameters used in the analysis. The second part will focus on the meshing technique employed, and the third part will present the results obtained.

### 3.1 Modeling Parameters

To enhance the accuracy of the results and reduce the simulation time, a two-dimensional geometry with a length of 2.5 cm and a thickness of 1 cm is applied in the plane

strain structural mechanics model. To characterize the impact of the laser, we implemented the force dipole model, which involves the application of two tangential forces with opposite directions on the surface [11]. The temporal evolution of the force dipole is expressed by the following Eq. 2, which corresponds to the temporal evolution of the heat source at the surface of the sample [10] :

$$F(t) = \frac{t}{\tau^2} \exp\left(\frac{-t}{\tau}\right) \cdot H(t) \quad (2)$$

Where :

H(t): Heaviside function,

$\tau$ : Durée d'impulsion laser.

The two parameters that are involved in this model are the width of the thermoelastic source, and the characteristic laser pulse duration.

### 3.2 Meshing

In order to obtain improved numerical results within a shorter simulation time, specific conditions must be applied to the meshing of the model. Considering  $f_{max}$  and  $\lambda_{min}$  the maximum acoustic frequency and the minimum wavelength respectively, the time step  $\Delta t$  and the size  $\Delta x$  of a mesh element must satisfy the following two equations in order to ensure the validity of the results obtained [1, 11].

Time step :

$$\Delta t < \frac{1}{20f_{max}} \quad (3)$$

Meshing element size :

$$\Delta x < \frac{\lambda_{min}}{20} \quad (4)$$

To satisfy Eq. 3 and Eq. 4, a fixed time step of 2 ns and a maximum element size of  $\Delta x = 8 \mu m$  are chosen, assuming a maximum acoustic frequency of approximately 18 MHz. A Perfectly Matched Layer (PML) with a fine mesh is used to effectively absorb both bulk and surface elastic waves, as illustrated in Figure 2.

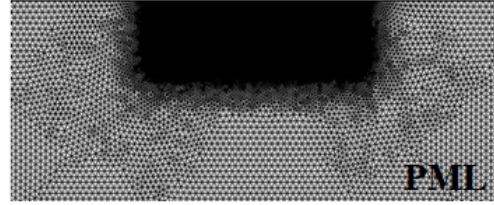


Figure 2. Meshing of an aluminum structure.

### 3.3 Results

Experimentally, multiple line sources with different energies is generated on the surface of an aluminum sample using optical devices. To validate the accuracy of the experimental results, a corresponding model is developed. This model consists of three line sources, each with a width of 200  $\mu m$  and separated by a distance of 3 mm, as shown in Figure 3.

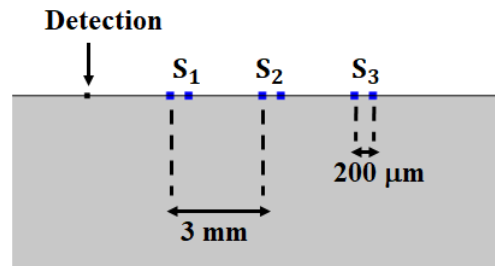
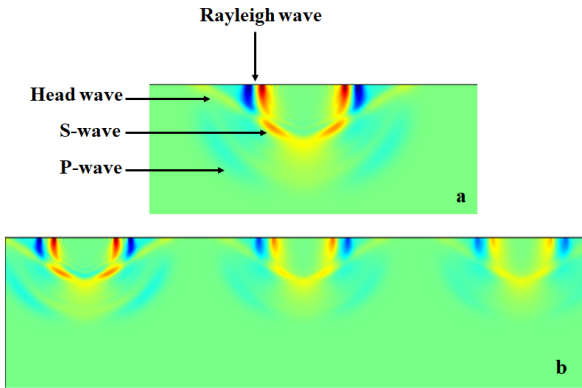


Figure 3. Diagram showing the positions of the three sources and the detection point.

Figure 4 (a) represents the propagation of multiple types of acoustic waves, such as longitudinal and shear waves, as well as head and Rayleigh waves, generated by line-focused laser pulse on a semi-infinite aluminum sample. The 2-D plot presented in Figure 4 (b) illustrates the results achieved by creating three dipolar sources, similar to those employed in the experimental study.

Each of the line sources generates a Rayleigh wave on the surface of the sample with a propagation velocity that depends on the material being considered. The normal displacement at the sample surface is detected and shown in Figure 5. From the signal, the propagation velocity of the Rayleigh wave can be calculated.



**Figure 4.** Results of 2-D finite element method for line-source (a) and multiple line sources (b) configurations.

The distance between the sources and the difference in time of flight between the echoes can be used to deduce a propagation velocity of  $2941 \text{ m/s}$ , which is consistent with the theoretical velocity obtained in paragraph 2.1.

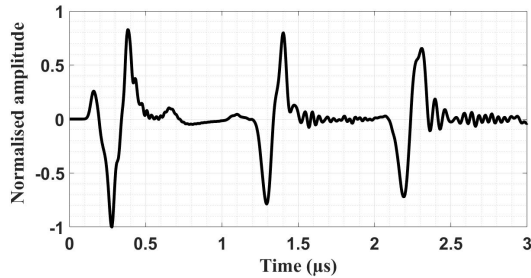


**Figure 5.** Signal representing the normal displacement associated to the Rayleigh waves generated by the three line sources.

As part of our modeling study, we incorporated a semi-circular form defect into the sample. The three sources,  $S_1$ ,  $S_2$  and  $S_3$ , are positioned on either side of the defect as illustrated in Figure 6.

The signals in figure 7 enable a comparison between the cases with and without the presence of a defect on the surface of the sample.

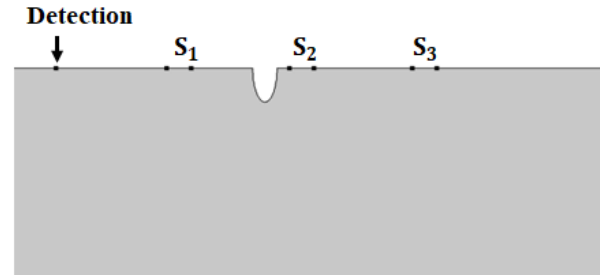


**Figure 6.** Sources, detection and defect configuration.

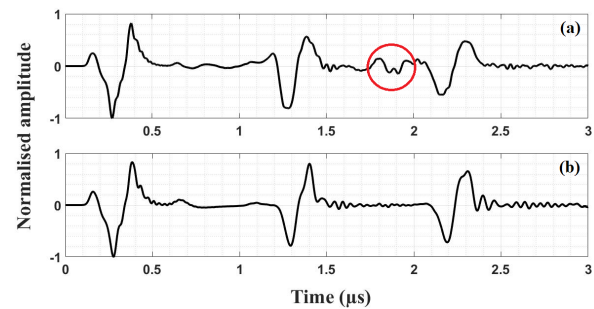


**Figure 7.** Signals obtained with (a) and without (b) a defect on the surface of the aluminum sample.

By comparing the two signals, a new echo is clearly observed in signal (a) that is representative of the interaction between the Rayleigh wave and the defect. This comparison enabled us to determine the flaw position.

## 4. EXPERIMENT

This section begins with a description of the experimental setup used. A comparative study of the effectiveness of using a single source versus multiple sources to measure the propagation velocity is presented. Finally, the sizing of the sample and positioning of the defect are discussed.

### 4.1 Procedure

An aluminum sample with a length of 9.9 cm and a thickness of 4.5 cm having a circular defect of 2.3 mm diameter is studied. A frequency-doubled Nd:YAG laser is employed, which produces a wavelength of 532 nm and emits pulses of approximately 10 nanoseconds. The laser beam passes through a diffraction grating with 600 lines/mm.



A cylindrical lens generates multiple thermoelastic line sources at the sample surface. Its normal displacement is detected using a Mach-Zehnder heterodyne interferometer. Figure 8 shows the experimental setup used.

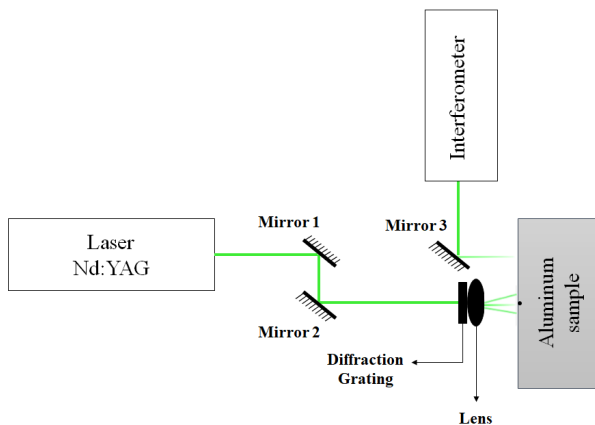


**Figure 8.** Experimental setup for generating and detecting surface acoustic waves by laser ultrasonics.

#### 4.2 Measurement of Rayleigh wave velocity.

In this section, a comparative study between the results obtained using a single and multiple linear sources is presented. In order to obtain the velocity of the Rayleigh wave, the time of flight needs to be measured, for which the propagation distance must be known. To accomplish this, the mirror 2 fixed on a motorized stage is moved in a controlled manner. The signals obtained before and after moving the mirror by a distance of 3 mm are shown in Figure 9.

According to the two signals in Figure 9, the time of flight difference is  $1.014 \mu\text{s}$ . This corresponds to a Rayleigh wave velocity of  $2958 \text{ m/s}$ . This velocity is coherent with both the theoretical velocity calculated in paragraph (2.1) and the velocity obtained through modeling in paragraph (3.3).

Having multiple equidistant line sources on the sample enables the generation of multiple Rayleigh waves, which allows the determination of the surface wave propagation velocity through two methods:

-The first method consists of considering the distance between sources for calculating the propagation velocity of the Rayleigh wave. It is then no longer necessary to proceed with mirror displacement, which can simplify the experimental setup and improve the measurement accuracy.

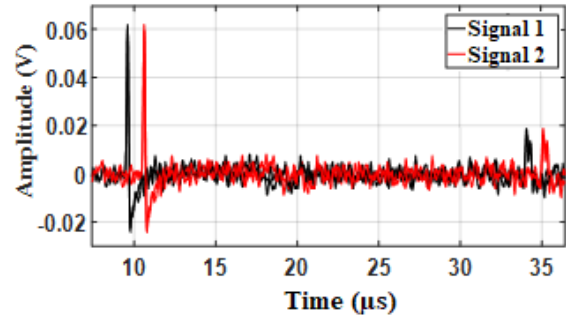


**Figure 9.** Signals obtained using a line source for two propagation distances separated by 3 mm.

-The second method consists of performing a displacement to detect a second signal as in the case of a single source. Indeed, obtaining three sources through the diffraction grating allows us to calculate three velocities of Rayleigh wave propagation and improve the measurement reliability. For this purpose, the diffraction grating is placed at a distance of 5.4 cm from the sample. Three line sources spaced of 1.7 cm are obtained. Figure 10 represents the signal associated to the Rayleigh waves generated by these three sources.

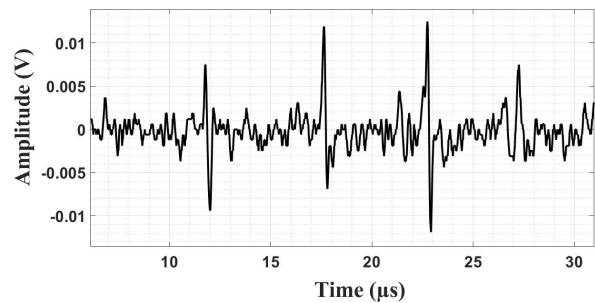


**Figure 10.** Signal associated to the Rayleigh waves generated by the three line sources.

From this signal, the propagation velocity of the Rayleigh wave is calculated using the first method. By knowing the distance between the sources and calculating the difference in time of flight between the obtained echoes, we deduce a propagation velocity of  $2890 \text{ m/s}$ . The second method of measuring the velocity requires a displacement of mirror 2, which causes a temporal shift in the obtained signal. Figure 11, represents the signals before and after a displacement of 3 mm.

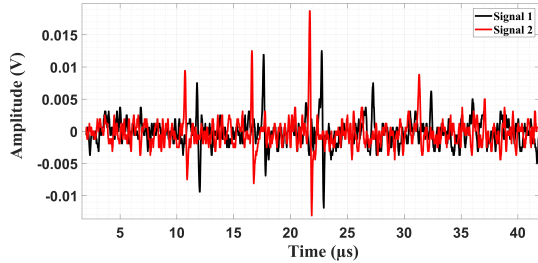


**Figure 11.** Signals obtained with three line sources for two propagation distances separated by 3 mm.

For a displacement of 3 mm, the difference in time of flight between echoes from the same source is 1.04  $\mu\text{s}$ . The propagation velocity of the Rayleigh wave deduced is equal to 2885 m/s.

The propagation velocities obtained for the different configurations are consistent. The multi-sources configuration can therefore be applied to non-destructive testing using surface acoustic waves for various structures.

### 4.3 Sample dimensions

The line sources obtained by the diffraction grating are distributed along the length of the sample. Considering the directivity of the Rayleigh wave associated to each source, it is possible to obtain the sample length and also to detect the defect. To determine the sample length, the sample and optical system are separated by 8.5 cm. The optical system enables the generation of three equidistant sources at the sample surface. Figure 12 shows the respective positions between the sources and the edges of the sample.

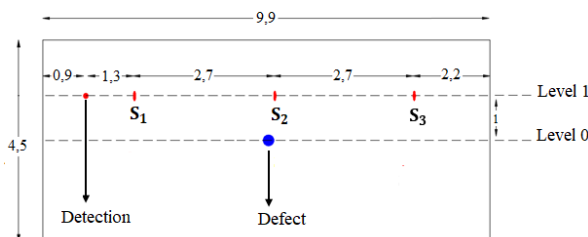


**Figure 12.** Diagram showing the positions of the three sources and the detection point at level 1. The distances on the diagram are in centimeter.

Each source has a width of approximately 0.5 mm and a

length of 2 mm. Figure 13 represents the signal obtained when the detection and line sources are aligned at level 1.

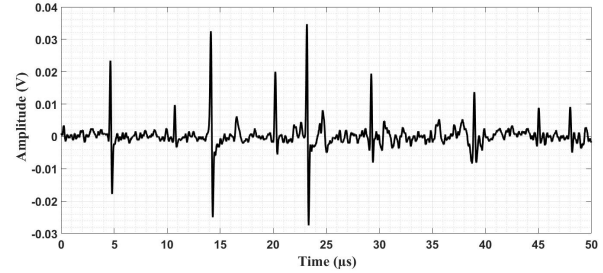


**Figure 13.** Signal detected at level 1 without defect.

In order to associate the signal echoes with the line sources, each source is masked. In Table 1, the time of flight and the distance between each source and the detection are provided. The propagation velocity of the considered Rayleigh wave is 2890 m/s, which corresponds to the one previously deduced from multiple sources without mirror displacement.

**Table 1.** Time of flight and propagation distance associated to the different sources.

Source	Duration ( $\mu\text{s}$ )	Distance ( $\mu\text{m}$ )
S <sub>1</sub>	4.64	1.37
S <sub>2</sub>	14.16	4.09
S <sub>3</sub>	23.28	6.73

Table 1 shows a good agreement between the calculated inter-source distance and the one measured experimentally, which is approximately 2.7 cm. We notice that the acquired signal contains several echoes associated to the reflections of Rayleigh waves by the edges of the sample. In order to identify the echoes associated to these reflections, masking sources S<sub>1</sub> and S<sub>3</sub> is performed. The masking of source S<sub>1</sub> allows us to deduce the distance between the detection and the left edge of the sample. Figure 14 shows the detected signals with and without source S<sub>1</sub>. We observe that when source S<sub>1</sub> is masked, two echoes are no longer present:

- The echo detected at 4.64  $\mu\text{s}$  is related to the path S<sub>1</sub>-detection,

- The echo detected at 10.72  $\mu\text{s}$  is related to the reflection

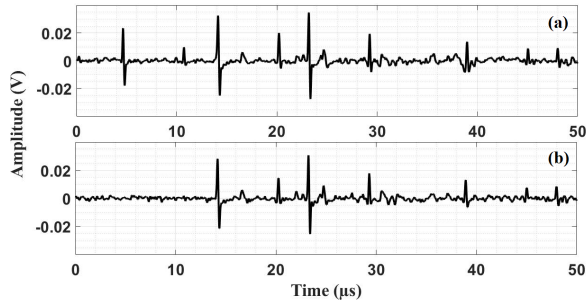


**Figure 14.** Signals detected with (a) and without (b)  $S_1$  source.

of the Rayleigh wave emitted by source  $S_1$  on the left edge of the sample. The difference in time of flight between these two echoes allows us to deduce that the distance between the detection and the left edge of the sample is approximately 0.9 cm.

Similarly, the masking of source  $S_3$  allows us to deduce the distance between the  $S_3$  and the right edge of the sample. Figure 15 shows the detected signals with and without source  $S_3$ .

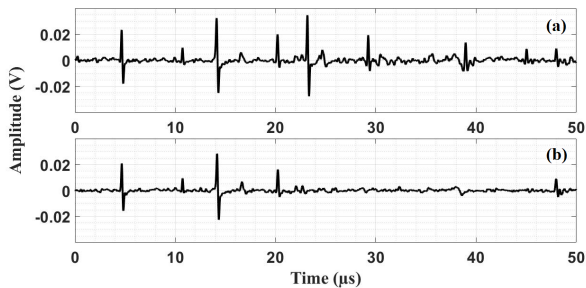


**Figure 15.** Signals detected with (a) and without (b)  $S_3$  source.

When source  $S_3$  is masked, three echoes are no longer present:

- The echo detected at  $23.28 \mu\text{s}$  corresponds to the  $S_3$ -detection path,
- The echo detected at  $29.24 \mu\text{s}$  corresponds to the reflection of the Rayleigh wave emitted by source  $S_3$  on the left edge of the sample,
- The echo detected at  $38.96 \mu\text{s}$  corresponds to the reflection of the Rayleigh wave emitted by source  $S_3$  on the right edge of the sample.

This allows us to deduce that the distance between source

$S_3$  and the right edge of the sample is approximately 2.27 cm, and the distance between the detection and the left edge is approximately 0.9 cm. Based on these results, the total length deduce of the sample is approximately 9.9 cm. Note that masking source  $S_2$  also confirms these results. The use of multiple line sources, each generating a Rayleigh wave on both sides of the source, allowed us to determine the length of the sample using the reflections of the different waves on the two edges of the sample. The distribution of several sources on the surface of the sample makes it possible to obtain signals of sufficient amplitude regardless of the chosen detection position.

#### 4.4 Defect location

The sample is vertically moved by 1 cm to place sources and the detection at level 0 as shown in Figure 16.

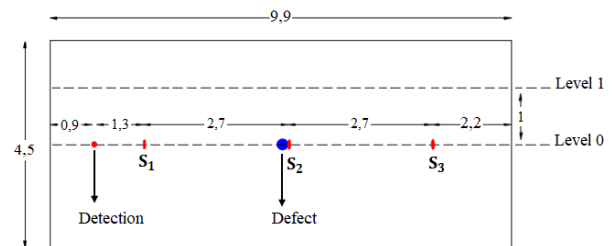


**Figure 16.** Diagram showing the positions of the three sources and the detection point at level 0. The distances on the diagram are in centimeter.

The three sources are positioned on either side of the defect. Figure 17 shows the signals in the case where detection and sources are at level 0 and at level 1.

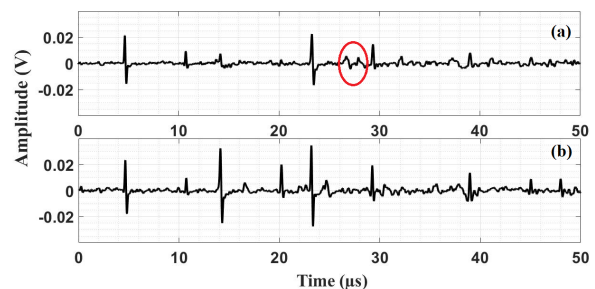


**Figure 17.** Signals detected at level 0 (a) and level 1 (b).

By comparing the two signals, it can be observed that:



-For source  $S_1$ , considering the temporal signal up to 12  $\mu\text{s}$ , there is no modification on the series of echoes of signal (a) compared to signal (b). There is therefore no defect on the associated paths.

-For source  $S_2$ , between 12  $\mu\text{s}$  and 21  $\mu\text{s}$ , there is a significant attenuation of the echo located at 14.16  $\mu\text{s}$  and corresponding to the direct path  $S_2$ -detection. The echo corresponding to the wave's reflection on the edge of the sample is almost entirely attenuated. This attenuation is characteristic of the interaction of the Rayleigh wave with the defect on the acoustic propagation path.

-For source  $S_3$ , around 22  $\mu\text{s}$ , we also observe the attenuation of the echo corresponding to the  $S_3$ -detection propagation path. This confirms the presence of the defect in this area of the sample.

In addition, a new echo (part circled in signal (a)) is observed. This echo is also clearly representative of the interaction of the Rayleigh wave with the defect. This shows that the waves emitted by each source and traveling through different paths make it possible to obtain significant information of each probed zone of the sample for NDT purpose.

Finally, the experimental results confirm the presence of an echo characterizing the defect as shown in the previously presented modeling in paragraph (3.3), which is clearly visible in Figures 17 and 7. However, determining the sample size precisely through modeling is not possible due to the PML layer, which prevents the visualization of reflection echoes on the sample's edges, such as those observed in the experimental results.

## 5. CONCLUSION

This study implements an optical device based on a diffraction grating to obtain multiple thermoelastic line sources. These sources allow the simultaneous excitation of Rayleigh waves traveling different paths. The spacing between the sources is determined by precisely positioning the sample surface at a certain distance from the optical system, which enables to obtain the Rayleigh wave velocity. By analyzing the different times of flight obtained for the excited waves, the length of the sample can be determined and a flaw easily detected without moving the sources. Furthermore, finite element modeling is used to predict waves-flaw interaction. The next objective of this study is to characterize the defect, dimensions and shape.

## 6. ACKNOWLEDGEMENTS

The authors would like to thank the Hauts- de- France region for the financial support provided in carrying out this study.

## 7. REFERENCES

- [1] C. Scruby and L. Drain, *Laser Ultrasonics Techniques and Applications*. Taylor & Francis, 1990.
- [2] J. Perdijon, *Le contrôle non destructif par ultrasons*. Hermes, 1993.
- [3] C. Pei, D. Yi, T. Liu, X. Kou, and Z. Chen, "Fully noncontact measurement of inner cracks in thick specimen with fiber-phased-array laser ultrasonic technique," *NDT & E International*, vol. 113, p. 102273, 2020.
- [4] L. Rayleigh, "On waves propagated along the plane surface of an elastic solid," *Proceedings of the London mathematical Society*, vol. 1, no. 1, pp. 4–11, 1885.
- [5] D. Royer and C. Chenu, "Experimental and theoretical waveforms of rayleigh waves generated by a thermoelastic laser line source," *Ultrasonics*, vol. 38, no. 9, pp. 891–895, 2000.
- [6] E. Dieulesaint and D. Royer, "Ondes élastiques dans les solides-tome 1: Propagation libre et guidée," 1996.
- [7] J. Rousseau, *Etude d'ondes de type Rayleigh sur des milieux stratifiés*. PhD thesis, 1979.
- [8] L. Beaujard, G. Labbe, and J. Mannenc, "Métallographie-essais non destructifs," *Encyclopaedia Universalis*, 2012.
- [9] F. Faëse, F. Jenot, M. Ouaftouh, and M. Duquennoy, "Ondes de rayleigh générées et détectées par laser—applications à la détection de défauts," *Proc. COFREND (Dunkirk)*, p. 141, 2011.
- [10] Y. Dai, B. Q. Xu, Y. Luo, H. Li, and G. D. Xu, "Finite element modeling of the interaction of laser-generated ultrasound with a surface-breaking notch in an elastic plate," *Optics & Laser Technology*, vol. 42, no. 4, pp. 693–697, 2010.
- [11] J. D. Achenbach, "Laser excitation of surface wave motion," *Journal of the Mechanics and Physics of Solids*, vol. 51, no. 11-12, pp. 1885–1902, 2003.